

Use of the cage formation probability for obtaining approximate phase diagrams

Atahualpa S. Kraemer¹ and Gerardo G. Naumis^{1,2,a)}

¹*Departamento de Física-Química, Instituto de Física, Universidad Nacional Autónoma de México (UNAM), Apartado Postal 20-364, 01000 Distrito Federal, Mexico*

²*Fac. de Ciencias, Universidad Autónoma de Morelos, Av. Universidad 10001, Cuernavaca, Morelos 62210, Mexico and Depto. de Física y Matemáticas, Universidad Iberoamericana, Av. Vasco de Quiroga 1, Santa Fé, 01000 Distrito Federal, México*

(Received 24 October 2007; accepted 27 February 2008; published online 7 April 2008)

In this work, we introduce the idea of cage formation probability, defined by considering the angular space needed by a particle in order to leave a cage given an average distance to its neighbors. Considering extreme fluctuations, two phases appear as a function of the number of neighbors and their distances to a central one: Solid and fluid. This allows us to construct an approximated phase diagram based on a geometrical approach. As an example, we apply this probability concept to hard disks in two dimensions and hard spheres in three dimensions. The results are compared with numerical simulations using a Monte Carlo method. © 2008 American Institute of Physics.

[DOI: [10.1063/1.2899732](https://doi.org/10.1063/1.2899732)]

I. INTRODUCTION

During the last decades, systems composed of hard-core particles (platelets, spheres, and rods) have been the subject of continuous and intense research,¹⁻⁷ since they are used as a benchmark tool in order to understand the behavior of simple fluids.¹ Recently, they gained a lot of attention due to the interest in colloids,⁸ nanostructured, granular media,^{4,7} disordered systems,^{9,10} and even in the assembly of virus capsids.¹¹ Old ideas were challenged, and for example, the concept of random close packing, which was considered as the paradigm of a disordered structure with nondirectional bonds,¹² was replaced with the idea of maximally random jammed state.⁵ A system is jammed when for all of the particles, it is not possible to move one without fixing the positions of all other particles. The concept of jamming has been proved to be very important,¹⁰ not only for practical reasons in granular media, but because is also relevant for hard-core potential and colloids. Also, it is related with the unsolved problem of the glass transition.¹³ More recently, the connection between jammed systems and low frequency vibrational modes has been explored,^{14,15} resulting in a possible explanation to the excess of low frequency modes in glasses,¹⁶ which are fundamental to determine the glass transition temperature.¹⁷ The dynamical formation of cages is another related concept which has been explored in connection to phase transitions. It is well known that the fluid-solid phase transition for hard spheres and hard disks (HPs) is due basically to the trapping of particles inside cages formed by its neighbors.¹⁸ When the packing fraction is diminished, the cages are open and a phase transition occurs.¹⁸ From a different point of view, the phase transition is entropically driven: Entropy is increased by forming cages.¹⁹ Some old theories assumed the formation of an underlying lattice with

cells, and the entropy was calculated by using free volume ideas.²⁰ However, the main problem is that cage formation is a collective effect, in which each particle is trapped by a cage and at the same time it forms the wall of a different cage. Later on, the density functional theory (DFT) was much more successful in predicting fluid-crystal phase transitions^{21,22} and was even able to anticipate the existence of quasicrystals.²³ Within DFT, a functional is build from some knowledge of the fluid properties.²⁴ Functionals for hard spheres²⁵ and HDs (Ref. 26) are available. The DFT can be improved by using some geometrical principles to construct a functional.²⁷ This approach leads to a very powerful method known as the fundamental measure theory.^{27,28} Furthermore, the DFT has been used to understand the formation and stability of hard-sphere glasses by Wolynes and co-workers.²⁹⁻³¹

In spite of the previous advances, not so much effort has been made in order to actually understand how dynamical cage formation is behind a fluid to solid transition, at least from a simple and transparent geometrical point of view. There are some previous efforts to study cage formation from the point of view of jamming,^{32,33} where there are contacts between particles. Here we adopt a different approach since we allow the particles to move inside the cages. We do this by using a mean field approach to understand how cages are related with the coordination number, average separation between particles, and packing fraction. Notice that in our mean field theory, we do not consider the strong coupling between angular and radial effects. The reason is that here we always adopt a worst case scenario approach, i.e., basically we provide bounds for the cage effect. Thus, here we will look at the most extreme angular fluctuations. So for example, if even in the most rare angular fluctuation a particle remains caged, then is clear that a fluidization cannot be observed. In reality, such extreme fluctuations are rare so the theory only provides a bound. However, our main objective

^{a)}Electronic mail: naumis@fisica.unam.mx.

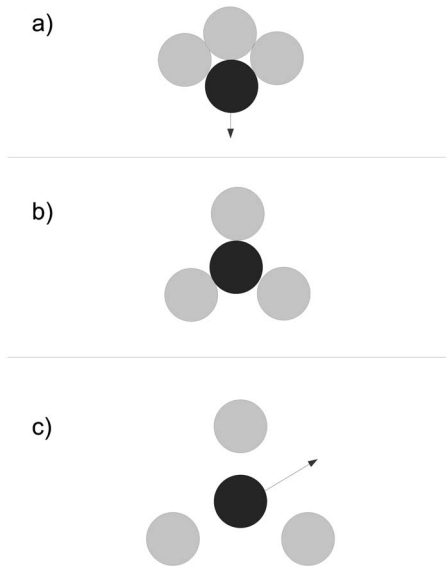


FIG. 1. A central particle and three neighbors. In (a), the central particle can leave the cage, as shown by the arrow. In (b), the neighbors trap the central particle, but if the distance of the first shell of neighbors is changed, as shown in (c), the cage is broken as indicated by the arrow.

here is to explore how far we can go using this simple mixing of geometrical arguments and extreme fluctuations compared with more sophisticated theories. By comparing with such theories, we can understand to what extent cage formation is behind a solid to fluid transition. Thus, the aim of this work is not the determination of where a transition occurs. There are much better theories to do this.²⁵ Instead we focus on how much such theories differ from assuming a simple mean field approach to cage formation. Eventually, this will clarify a hierarchy of important aspects in the phenomena of cage formation. This mean field approximation does not give information about the long-range order nature of the solid phase. This approach is developed in Sec. II by defining a cage formation probability. The idea is tested for a HD system, and then it is extended in Sec. III to hard spheres. Finally, the conclusions and perspectives are given in Sec. IV.

II. CAGE FORMATION PROBABILITY IN TWO DIMENSIONS

In this section, we will define the concept of cage formation probability. To start, let us consider the most simple case: A system of HDs. Take any HD at random. Such disk will be surrounded by Z first neighbors, where Z can be determined using different methods such as a Voronoi polyhedra or using the radial distribution function. For such disk, which we will call central, there are two possibilities: It can be trapped inside a cage produced by these Z neighbors, or it can leave the cage if enough space is available to do so. For the first case, there are also two possibilities: The particle can be jammed or it can be moved inside the cage. The trapping effect depends crucially in the lack of available space needed by a particle in order to leave the cage. However, the geometry of the available space is also important. For example, in Fig. 1 we show a HD in contact with three other disks. In Fig. 1(a), the central disk can leave the cage while in

Fig. 1(b) is trapped. In both cases, the sum of the angular sectors not covered by the neighbors is the same. If one considers all possible angular distributions of the surrounding three disks, only when they form an equilateral triangle the central will be jammed. In a pure HD fluid, the possibility of such perfect configuration is remote compared with other distributions of the disks. Our example shows the fundamental relationship between orientational order and caging. As we observe in Fig. 1(c), the distance between the central one and the first shell of neighbors also affects the cage effect, since if the triangle of Fig. 1(b) is expanded, the central particle will eventually leave the cage. Notice how in our line of argumentation, we are supposing that all these Z neighbors are at the same distance. This is of course not true for real fluids. However, from the fact that there is a first peak in the pair distribution function $g(r)$, one can assume that the distance of the neighbors is on average given by this peak with a dispersion around a given value. This average distance will be denoted by $\langle r \rangle$.

The previous discussion shows that two ingredients are responsible for caging, one is the distance from the first shell of neighbors and the second their angular configuration. In a fluid, the cage effect is time dependent, in contrast with the previous discussion. However, it is known that when a fluid approaches a transition to a solid, the local structural arrest can be described in terms of averaged quantities.³⁴ This suggests to define a probability that Z neighbors cage a fixed particle j . If $\langle r \rangle$ is the average distance from j to the first shell of neighbors, such probability can be defined as follows:

$$p_{j,Z}(\langle r \rangle) \equiv \frac{\Omega_j^c(Z, \langle r \rangle)}{\Omega_j(Z, \langle r \rangle)}, \quad (1)$$

where $\Omega_j^c(Z, \langle r \rangle)$ is the number of angular configurations in which the particle j is caged by Z neighbors at an average distance $\langle r \rangle$, while $\Omega_j(Z, \langle r \rangle)$ is the total number of configurations available with the same fixed Z and $\langle r \rangle$. The quantity $\Omega_j^c(Z, \langle r \rangle)$ can be interpreted as the phase space contribution of a local cage, compared with $\Omega_j(Z, \langle r \rangle)$ which is the phase volume accessible to the local configuration. One can obtain $\Omega_j(Z, \langle r \rangle)$ using configurational integrals on the angular sectors as follows:³³

$$\begin{aligned} \Omega_j(Z, \langle r \rangle) &= \int d\omega_1 \int d\omega_2 \cdots \int d\omega_Z \delta \\ &\times \left(\sum_{j=1}^Z \omega_j - 2\pi \right) \Theta(\omega_1 - \varphi) \\ &\Theta(\omega_2 - \varphi) \cdots \Theta(\omega_Z - \varphi), \end{aligned} \quad (2)$$

where ω_i is the angle between the neighbor i of particle j and the next one taken in a counterclockwise direction, φ is the minimal separation angle between hard-core neighbors as shown in Fig. 2(b), $\delta(x)$ is the Dirac delta function that assures that the sum of all angles is 2π , and $\Theta(x)$ is the theta function which takes value zero if $x \leq 0$ and one otherwise. The corresponding number of caged configurations is just obtained by observing that a particle is not caged whenever

the free angular space is such that for at least one ω_1 it is observed that $\omega_1 > \pi$, from where it follows that

$$\begin{aligned} \Omega_j^c(Z, \langle r \rangle) &= \Omega_j(Z, \langle r \rangle) - \int d\omega_1 \int d\omega_2 \cdots \int d\omega_Z \delta \\ &\times \left(\sum_{j=1}^Z \omega_j - 2\pi \right) \Theta(\omega_1 - \varphi) \\ &\Theta(\omega_2 - \varphi) \cdots \Theta(\omega_Z - \pi). \end{aligned} \quad (3)$$

The caging probability allows us to construct a diagram in Z and $\langle r \rangle$ observing the following.

- (1) If $p_{j,z}(\langle r \rangle) = 0$ for all particles, the system is for sure fluid.
- (2) If $0 < p_{j,z}(\langle r \rangle) < 1$, the fluid can be in coexistence with the solid.
- (3) If $p_{j,z}(\langle r \rangle) = 1$ for all particles, the system is for sure a solid.

Consider condition 1. For having a fluid, it is required a zero cage probability: This happens if even in the best trapping configuration of the cage, the central disk has the opportunity to leave it after a long time. The best possible trap is the configuration in which the exterior shell forms a regular polygon, since all the available free space is distributed equally and thus all “holes” in the cage are repaired [see Fig. 1(b)]. However, if this best trapping configuration is expanded, as in Fig. 1(c), there is a critical distance at which one needs to put a new particle in the shell to have the cage effect, since the holes are so big that they are not able to block the central particle. Using the cosine law applied for regular polygons [see Figs. 1(b) and 1(c)], this critical radius $\langle r \rangle$ is related with the minimal Z required to have at least the possibility to cage,

$$\langle r \rangle = \sigma \sqrt{\frac{2}{1 - \cos(2\pi/Z)}}. \quad (4)$$

The inverse of this equation gives the coordination as a function of the radius for which there is a transition from a “sure” fluid (condition 1) to condition 2. The other possible transition is from a sure solid (case 3) to case 2, so we need to proceed in the opposite direction.

Thus, consider now condition 3. To have the particle in a cage with probability one, we need to assure that even for the best escaping configuration of disks, the particle will be trapped. Such best escape configuration, created by a rare fluctuation, is obtained when all the available free space is used to produce a big hole, as shown in Fig. 2. This big hole is made by joining all the disks in the surrounding shell in such a way that they produce a chain of disks in contact. Again, it is clear that such escape configuration is only able to work up to a certain radius, since at a bigger one a new neighbor is needed to repair the hole. Thus, there is a relationship between the minimal number of neighbors required to trap a particle and a certain radius. Now we will calculate such relationship. By calling φ to the angle defined by the

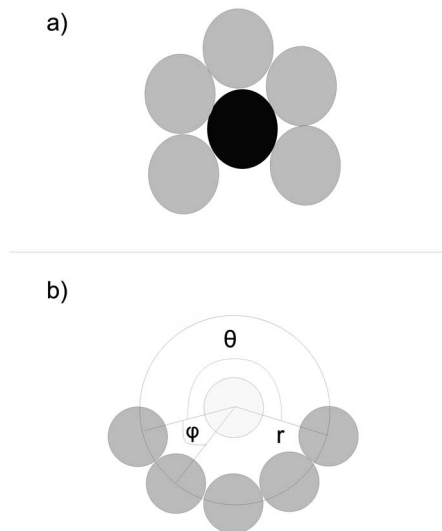


FIG. 2. In (a) the central particle is trapped, but as the configuration is expanded, it reaches a point in which there is enough room for the central particle to escape. The critical radius at which such escape occurs is given by Eq. (6).

central particle and the two contiguous disks in the chain (see Fig. 2), the maximal distance $\langle r \rangle$ for which the caging works is given by

$$\varphi = 2 \sin^{-1} \left(\frac{\sigma}{2\langle r \rangle} \right). \quad (5)$$

Using that the angular size of the hole (θ) is related with φ as $\theta = 2[\pi - (Z-1)\varphi]$, we obtain the following transcendental equation:

$$\langle r \rangle = \sigma \sqrt{\frac{2}{1 - \cos(2[\pi - (Z-1)2 \sin^{-1}(\sigma/2\langle r \rangle)])}}, \quad (6)$$

which can be solved by using an iterative procedure. As a result, one gets the minimal number of neighbors required to cage a particle for a given distance. The resulting plot is shown as a line in Fig. 3. The region $p_{j,z}(\langle r \rangle) = 1$ is indicated with the word “solid,” where the average coordination of the particles is defined as

$$\langle Z \rangle = \frac{1}{N} \sum_{j=1}^N Z_j, \quad (7)$$

which is taken equal to $\langle Z \rangle = Z$, since we assume that all neighborhoods of the particles are almost similar.

Equation (6) produces the geometrical phase diagram shown in Fig. 3, in which the average distance between neighbors gives the required coordination needed to form a cage. This diagram can be compared with the results obtained from a simulation. To do so, we made Monte Carlo simulations for a system of 100 HDs using an NVT ensemble at different packing fractions $\phi = N\pi\sigma^2/4S$, where S is the area of the simulation box and N is the number of particles. Once the systems were equilibrated, the radial distribution function $g(r)$ was calculated. The average coordination of the lattice was obtained from

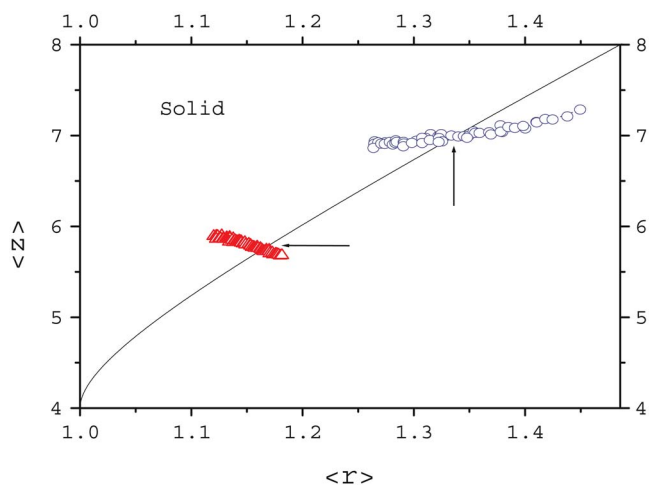


FIG. 3. (Color online) Minimal number of neighbors $\langle Z \rangle$ required to cage a particle as a function of the average distance $\langle r \rangle$ to the first neighbors. The solid line separates the region where the system is solid, and the zone where there is an escape probability different from zero. The solid line was obtained by solving Eq. (6). The symbols represent the evolution of a Monte Carlo simulation using 100 disks. For the triangles, $\langle r \rangle$ was obtained using as cutoff (r_c) the first minimum of $g(r)$. The circles were obtained from $g^*(r)$ as described in the text. The arrows indicate the intersection points with the solid line, corresponding to $\phi=0.674$ and $\phi=0.709$ for the triangles and circles, respectively.

$$\langle Z \rangle = 2\pi \int_0^{r_c} g(r)rdr, \quad (8)$$

where r_c is a cut-off radius used to determine the end of the first shell of neighbors. There are several possible criteria to do this: Voronoi polyhedra, the first local minimum of $g(r)$, or the contact region.⁹ $\langle r \rangle$ can be calculated from $g(r)$ in a consistent way with the criteria used to determine r_c . In general, $\langle r \rangle$ can be calculated from

$$\langle r \rangle = \frac{\int_0^{r_c} g(r)r^2 dr}{\int_0^{r_c} g(r)rdr}. \quad (9)$$

In Fig. 3 we present the results of the simulation using as cutoff r_c the first minimum of $g(r)$. Each triangle corresponds to a pair of Z and $\langle r \rangle$ for a given ϕ . Starting with $\langle Z \rangle \approx 6$ and $\langle r \rangle \approx 1.1$, the system evolves as the lattice is expanded and $\langle Z \rangle$ decreases. According to the diagram, the end of the solid region is obtained by the intersection of the condition given by Eq. (6), and the evolution of the system, denoted by triangles. The intersection obtained is $\phi=0.674$, which is below the known melting point for HDs, at⁸ $\phi_c \approx 0.72$. Although the error is about 6.4%, it shows that the geometrical criteria provide a rough estimation of the melting point, and it gives a simple picture based in the cage effect. Notice that we compare with the melting point because in our line of thought we considered a solid in which all the particles were caged. Then, as the density decreases, there is a certain point in which caging is impossible even in the best trapping configuration. Thus it is impossible to hold a solid under such condition.

As stated previously, there is a certain degree of ambiguity in the cut-off criteria. It is natural to ask how the results depend upon such election, and if there is any way to im-

prove the estimation of $\langle r \rangle$. We proceed as follows: First, observe that for a given r , $g(r)$ contains contributions from different shells of neighbors. One can remove such contributions by deconvoluting $g(r)$ using, for example, Lorentzians of the type

$$f(r) = \frac{A_n(\phi)}{B_n(\phi) + (r - r_n(\phi))^2},$$

where $A_n(\phi)$ and $B_n(\phi)$ are fitting constants, and $r_n(\phi)$ is the position of the peak with label n , starting with $n=1$ for the first peak of $g(r)$, $n=2$ for the second, and so on. Notice that the position of each peak depends upon the packing fraction. Using the proposed deconvolution, a new $g^*(r)$ can be defined by

$$g^*(r) = \frac{A_0(\phi)}{B_0(\phi) + r^2}.$$

Using $g^*(r)$, $\langle Z \rangle$ and $\langle r \rangle$ are easily obtained from Eqs. (8) and (9) by replacing $g(r)$ with $g^*(r)$ and $r_c \rightarrow \infty$. The resulting evolution of $\langle Z \rangle$ vs $\langle r \rangle$ is displayed in Fig. 3, showing a higher coordination for a given r . This seems to be paradoxical, because the contribution from the second shell was removed. However, a detailed analysis shows that, in fact, such increased coordination is due to the different cut-off. The calculation of $\langle Z \rangle$ and $\langle r \rangle$ with $g(r)$ uses a cutoff at the first minima, while $g^*(r)$ is integrated to a high r_c . The intersection between this correction and Eq. (6) occurs at $\phi=0.704$, which gives a much better approximation, with an error of 2.3%.

Also, the geometrical cage diagram can be used to get information about the nature and stability of the lattices. For example, from Fig. 3 is clear that the first solid lattice appears for $\langle Z \rangle=4$. However, the resulting lattice must be disordered, since from Fig. 3, for $\langle Z \rangle=4$ the disks are in contact, and a configuration with a central disk caged by four neighbors forming a perfect square is unstable. A slight angular displacement of the perfect square cage will produce enough free space for the central disk to leave the cage. It is worthwhile mentioning that such disordered arrangement will be basically jammed, since the particles are in contact. It is known that disordered packing of disks or spheres are isostatic in the sense of rigidity.³⁵ A lattice is isostatic when the number of mechanical contacts (N_c) is equal to the number of degrees of freedom in the configurational space (N_D). In D dimensions, $N_D=DN$. Since each contact is shared by two disks or spheres, in a mean field approximation $N_c \approx \langle Z \rangle N/2$. Applying the isostatic condition $N_c=N_D$, we have that $\langle Z \rangle \approx 2D$. For two dimensions $\langle Z \rangle \approx 4$. This number is in agreement with the one obtained by our simple geometrical approach. Other disordered packings are possible with different coordination numbers, but $g(r)$ is not regular and a well defined first shell is difficult to extract.³⁶ It is important to remark that our approach does not allow us to distinguish between crystalline and amorphous phases, since it does not take into account long-range information. However, geometry still provides some tentative answers. For example, a crystal can be obtained for $\langle Z \rangle=6$, while it is not possible to have a periodic arrangement with $\langle Z \rangle=5$.

Finally, Fig. 3 allows us to obtain the approximate packing fraction of the melting point using pure geometrical arguments, without using numerical simulations. From the previous discussion, we can speculate about the formation of a crystalline lattice by local caging. According to Fig. 3, the solid can only exist for $\langle Z \rangle = 6$ when $1 \leq \langle r \rangle \leq 1.19$. The maximal expanded hexagonal lattice occurs at $\langle r \rangle \approx 1.19$. Thus a transition to a no-caging condition happens if $\langle r \rangle > 1.19$. Using that the packing fraction for a hexagonal lattice with lattice constant $\langle r \rangle$ is

$$\phi = \frac{\pi}{2\sqrt{3}\langle r \rangle^2}, \quad (10)$$

we obtain that $\phi \approx 0.64$, a value that underestimates ϕ_c by 11%. Such prediction requires only two simple equations, Eqs. (6) and (10). Thus, simple geometric arguments are able to locate the approximate location of the solid melting point. The difference with the real value arises in the widening of the peaks in $g(r)$, which leads to fluctuations in $\langle r \rangle$, and the radial-angular coupling effects.

III. A THREE DIMENSIONAL CASE: HARD SPHERES

In this section, we show how to extend the present approach to the case of three dimensions. As an example, we explore the cage diagram of hard spheres with diameter σ . Following the path developed for HDs, the first ingredient is the identification of densities in which all spheres are trapped in cages with probability 1. This can be done considering a central sphere and a first neighbor sphere at distance $\langle r \rangle$. This first neighbor, due to the hard-core repulsion potential, excludes an area A_{exc} to the central particle. The area available for the central particle to leave the cage is the area of a sphere with radius $\langle r \rangle$ minus the excluded volume by its first neighbor,

$$A_{eff} \equiv 4\pi\langle r \rangle^2 - A_{exc}, \quad (11)$$

where A_{exc} is the area of a spherical cap,

$$A_{exc} = \langle r \rangle^2 \int_0^{2\pi} \int_0^\beta \sin \theta d\theta d\varphi = 2\pi\langle r \rangle^2(1 - \cos \beta), \quad (12)$$

and β is the arc defined by the first neighbor sphere as seen from the central particle,

$$\beta = \sin^{-1}\left(\frac{\sigma}{2\langle r \rangle}\right). \quad (13)$$

When $\langle Z \rangle$ neighbors are present, the area available can be written as a first approximation just by considering that each sphere excludes an area A_{exc} ,

$$A_{eff} \approx 4\pi\langle r \rangle^2 - \langle Z \rangle A_{exc}. \quad (14)$$

A solid is obtained when $A_{eff} < A_{exc}$ since there is not available space for the central particle to leave the cage. The separatrix between the solid and the fluid is thus given by

$$4\pi\langle r \rangle^2 - (\langle Z \rangle + 1)A_{exc} \approx 0. \quad (15)$$

By feeding Eq. (15) with A_{eff} as given by Eqs. (12) and (13), we obtain that

$$\left(2 - (\langle Z \rangle + 1) \left[1 - \cos \sin^{-1}\left(\frac{\sigma}{2\langle r \rangle}\right)\right]\right) \approx 0. \quad (16)$$

However, the previous equation is valid only in a mean field sense, since the excluded volume must take into account two things: The central particle must be caged even for the configurations of neighbors that let the maximal open space on the sphere of radius $\langle r \rangle$, and in such configurations, there are contacts between the neighbors. The configurations that produce a maximal open space consist in putting all the spheres of the shell in a maximal packing arrangement. Since the intersection of a shell of radius $\langle r \rangle$ with a sphere produces a disk, this problem turns out to be similar to the problem of finding the optimally close packed coverage of a sphere with disks. In the mathematical literature, such question is known as the Tammes problem.³⁷ Results are available for small numbers of disks in an exact or numerical form.³⁸ Using these ideas, the total excluded area must be replaced by

$$A_{exc} \rightarrow A_{exc} \phi_T(\langle Z \rangle + 1), \quad (17)$$

where $\phi_T(N)$ is the packing fraction of Tammes for N disks in a sphere. $\phi_T(N)$ oscillates between³⁸ 0.9 and 0.78. The new excluded area can be inserted into Eq. (16) which is finally written as

$$\left(2 - \frac{(\langle Z \rangle + 1)}{\phi_T(\langle Z \rangle + 1)} \left[1 - \cos \sin^{-1}\left(\frac{\sigma}{2\langle r \rangle}\right)\right]\right) \approx 0. \quad (18)$$

Equation (18) has solutions for $\langle r \rangle \geq \sigma$ only for $\langle Z \rangle > 10$. For $\langle Z \rangle = 11$, $\langle r \rangle = \sigma$ and for $\langle Z \rangle = 12$, $\langle r \rangle = 1.053\sigma$. Since there are not regular lattices with $\langle Z \rangle = 11$, we can assume that a solid with $\langle Z \rangle = 12$ is the one to be formed, which we can speculate that it corresponds roughly to a fcc structure. The packing fraction of a fcc structure with lattice parameter $\langle r \rangle$ is given by

$$\phi = \frac{\sqrt{3}\pi}{8} \left(\frac{\sigma}{\langle r \rangle}\right)^3. \quad (19)$$

According with the present approach, cages begin to be broken at $\langle r \rangle = 1.053\sigma$ and thus melting happens at $\phi_m \approx 0.582$. This value is 6.8% higher than the one obtained from other sources, which report³⁹ $\phi_m \approx 0.545$. Notice that we compare with the melting point because our line of reasoning is the following: When the system is dense packed, all cages are not destroyed even by the biggest available angular fluctuation. The system is thus a solid. When ϕ decreases, angular fluctuations that are able to destroy cages appear at $\langle r \rangle = 1.053\sigma$ and thus some fluidization is possible. This corresponds to melting. It is also worthwhile mentioning that hard-sphere numerical simulations tend to slow down at $\phi \approx 0.58$, which is usually associated with the formation of a glass.³⁹ At the moment, the origin of the coincidence between the value obtained with the geometrical approach and the onset of glass transition is not clear. The glass transition is a kinetic crossover and here we do not have access to the dynamics, so making any possible connection is for the moment a speculation.

IV. CONCLUSIONS

In conclusion, we have shown that the escape probability of a caged particle can serve as a tool to develop a kind of phase diagram based in pure geometric considerations. Using these ideas, it is possible to deduce the approximate location of the melting point. For HDs, the melting point was located within 11% from the accepted value, while for hard spheres it gives 6.8%. In this last case, the value seems to coincide with the place where the glass transition appears, but maybe this is just a coincidence. For the moment the method is not very accurate, but instead it sheds some light in the process of cage formation, a fact that is usually obscured in more sophisticated treatments of the problem. In future works, we will use molecular dynamics to test the idea of escape probability using a study of the distribution of dynamic contacts, and the relationship with the orientational order parameters, which is an essential ingredient to improve the ideas presented in this work.

ACKNOWLEDGMENTS

This work was supported by DGAPA UNAM Project Nos. IN108502, IN111906, and CONACyT 48783-F, 50368.

¹B. J. Alder and T. E. Wainwright, *Phys. Rev.* **127**, 359 (1962).

²A. P. Gast, C. K. Hall, and W. B. Russell, *J. Colloid Interface Sci.* **96**, 251 (1983).

³H. Weber, D. Marx, and K. Binder, *Phys. Rev. B* **51**, 14636 (1995).

⁴A. Mehta and G. C. Barker, *Phys. Rev. Lett.* **67**, 394 (1991).

⁵S. Torquato, T. M. Truskett, and P. G. Debenedetti, *Phys. Rev. Lett.* **84**, 2064 (2000).

⁶T. M. Truskett, S. Torquato, and P. G. Debenedetti, *Phys. Rev. E* **62**, 993 (2000).

⁷V. Tohver, A. Chan, O. Sakurada, and J. A. Lewis, *Langmuir* **17**, 8414 (2001).

⁸A. Huerta, G. G. Naumis, D. T. Wasan, D. Henderson, and A. Trokhymchuk, *J. Chem. Phys.* **120**, 1506 (2004).

⁹A. Huerta and G. G. Naumis, *Phys. Rev. Lett.* **90**, 145701 (2003).

¹⁰P. Chaikin, *Phys. Today* **60**(6), 8 (2007).

¹¹T. Chen, Z. L. Zhang, and S. C. Glotzer, *Proc. Natl. Acad. Sci. U.S.A.* **104**, 717 (2007).

¹²R. Zallen, *The Physics of Amorphous Solids* (Wiley, New York, 1983).

¹³A. J. Liu and S. R. Nagel, *Nature (London)* **396**, 21 (1998).

¹⁴A. Huerta and G. G. Naumis, *Phys. Lett. A* **299**, 660 (2002).

¹⁵A. Huerta and G. G. Naumis, *Phys. Rev. B* **66**, 184204 (2002).

¹⁶G. G. Naumis, *Phys. Rev. E* **71**, 026114 (2005).

¹⁷G. G. Naumis, *Phys. Rev. B* **73**, 172202 (2006).

¹⁸X. Z. Wang, *J. Chem. Phys.* **122**, 044515 (2005).

¹⁹A. P. Gast and W. B. Russel, *Phys. Today* **51**(12), 24 (1998).

²⁰W. G. Hoover and B. J. Adler, *J. Chem. Phys.* **46**, 686 (1967).

²¹S. Alexander and J. P. McTague, *Phys. Rev. Lett.* **41**, 702 (1978).

²²T. V. Ramakrishnan and M. Yussouff, *Phys. Rev. B* **19**, 2775 (1975).

²³P. M. Chaikin and T. C. Lubensky, *Principles of Condensed Matter Physics* (Cambridge University Press, Cambridge, 2000).

²⁴J. A. Capitán and J. A. Cuesta, arXiv:0704.2379v.

²⁵P. Tarazona, *Phys. Rev. A* **31**, 2672 (1985).

²⁶A. Esztermann, H. Reich, and M. Schmidt, *Phys. Rev. E* **73**, 011409 (2006).

²⁷Y. Rosenfeld, *Phys. Rev. Lett.* **63**, 980 (1993).

²⁸S. Phan, E. Kierlik, M.-L. Rosinberg, B. Bildstein, and G. Kahl, *Phys. Rev. E* **48**, 618 (1993).

²⁹P. G. Wolynes, *J. Non-Cryst. Solids* **75**, 443 (1985).

³⁰Y. Singh, J. P. Stoessel, and P. G. Wolynes, *Phys. Rev. Lett.* **54**, 1059 (1985).

³¹R. W. Hall and P. G. Wolynes, *J. Chem. Phys.* **86**, 2943 (1987).

³²E. A. J. F. Peters, M. Kollmann, M. A. O. M. Barenbrug, and A. P. Philipse, *Phys. Rev. E* **63**, 021404 (2001).

³³A. Wouterse, M. Plapp, and A. P. Philipse, *J. Chem. Phys.* **123**, 054507 (2005).

³⁴K. Binder and W. Kob, *Glassy Materials and Disordered Solids* (World Scientific, Singapore, 2005).

³⁵C. F. Moukarzel, *Phys. Rev. Lett.* **81**, 1634 (1998).

³⁶A. R. Kansal, T. M. Truskett, and S. Torquato, *J. Chem. Phys.* **113**, 4844 (2000).

³⁷H. Coxeter, *Trans. N. Y. Acad. Sci.* **24**, 320 (1962).

³⁸B. W. Clare and D. L. Kepert, *Proc. R. Soc. London, Ser. A* **405**, 329 (1986).

³⁹P. Chaikin, *Soft and Fragile Matter* (Institute of Physics, London, 2000).